Selectivity and Gating of the Type *L* Potassium Channel in Mouse Lymphocytes

MARK S. SHAPIRO and THOMAS E. DECOURSEY

From the Department of Physiology, Rush Presbyterian St. Luke's Medical Center, Chicago, Illinois 60612

ABSTRACT Type *l* voltage-gated K^+ channels in murine lymphocytes were studied under voltage clamp in cell-attached patches and in the whole-cell configuration. The kinetics of activation of whole-cell currents during depolarizing pulses could be fit by a single exponential after an initial delay. Deactivation upon repolarization of both macroscopic and microscopic currents was mono-exponential, except in Rb-Ringer or Cs-Ringer solution in which tail currents often displayed "hooks," wherein the current first increased or remained constant before decaying. In some cells type *l* currents were contaminated by a small component due to type *n* K^+ channels, which deactivate ~10 times slower than type *l* channels. Both macroscopic and single channel currents could be dissected either kinetically or pharmacologically into these two K^+ channel types. The ionic selectivity and conductance of type *l* channels were studied by varying the internal and external permeant ion. With 160 mM K^+ in the cell, the relative permeability calculated from the reversal potential with the Goldman-Hodgkin-Katz equation was K^+ ($\equiv$1.0) > Rb^+ (0.76) > NH_4^+ = Cs^+ (0.12) $\gg$ Na^+ (<0.004). Measured 30 mV negative to the reversal potential, the relative conductance sequence was quite different: NH_4^+ (1.5) > K^+ ($\equiv$1.0) > Rb^+ (0.5) > Cs^+ (0.06) $\gg$ Na^+, Li^+, TMA^+ (unmeasurable). Single channel current rectification resembled that of the whole-cell instantaneous *I-V* relation. Anomalous mole-fraction dependence of the relative permeability P_{NH_4}/P_K was observed in NH_4^+-K^+ mixtures, indicating that the type *l* K^+ channel is a multi-ion pore. Compared with other K^+ channels, lymphocyte type *l* K^+ channels are most similar to "g_{f2}" channels in myelinated nerve.

INTRODUCTION

Three types of voltage-gated delayed rectifier–type K^+ channels have been described in lymphocytes, which have been named type *n*, type *l* (DeCoursey et al., 1987*a*), and type *n'* (Lewis and Cahalan, 1988). Type *n* channels, the dominant delayed rectifier

Address reprint requests to Dr. Thomas E. DeCoursey , Dept. of Physiology, Rush Presbyterian-St. Luke's Medical Center, 1653 West Congress Parkway, Chicago, IL 60612.

Dr. Shapiro's present address is Department of Physiology/Biophysics, University of Washington, SJ-40, Seattle, WA 98195.

J. GEN. PHYSIOL. © The Rockefeller University Press · 0022-1295/91/06/1227/24 $2.00
Volume 97 June 1991 1227–1250

K^+ channel in most human (DeCoursey et al., 1984; Matteson and Deutsch, 1984; Cahalan et al., 1985) and murine lymphocytes (Chandy et al., 1986; DeCoursey et al., 1987*b*), resemble delayed rectifier channels in skeletal muscle and some neurons in many respects, including ionic selectivity and a fivefold slowing by external Rb^+ of deactivation kinetics (Cahalan et al., 1985). Taking into account all known properties, type *l* channels most closely resemble the g_{f2} component of delayed rectifier currents in frog (Dubois, 1981*b*; Plant, 1986; Jonas et al., 1989) and rat (Röper and Schwarz, 1989) node of Ranvier (compare Shapiro, 1990). Type *l* channels are easily differentiated from type *n* or type *n'* channels on the bases of kinetics, voltage dependence, single channel conductance, and sensitivities to TEA^+ (DeCoursey et al., 1987*a*, *b*; Lewis and Cahalan, 1988) and charybdotoxin (Sands et al., 1989).

Type *l* channels were first described in a subset of T lymphocytes from MRL-*lpr/lpr* mice, in which they are the dominant ionic conductance and are present in large numbers (Chandy et al., 1986; DeCoursey et al., 1987*a*). This murine strain has a single gene locus mutation that gives rise to a disease resembling human systemic lupus erythematosus, and displays a hundred-fold polyclonal lymphoproliferation of a functionally and phenotypically ($CD4^-$ $CD8^-$ $B220^+$) abnormal subset of T cells (Altman et al., 1981; Murphy, 1981; Wofsy et al., 1981). Type *l* channels are also found in some T lymphocytes from normal mice (DeCoursey et al., 1987*b*), in a fraction of rat type II alveolar epithelial cells (DeCoursey et al., 1988), in normal suppressor-precursor ($CD4^-$ $CD8^+$) murine thymocytes (Lewis and Cahalan, 1988), and in the *Louckes* human lymphoma cell line (Shapiro and DeCoursey, 1988).

Although several properties of type *l* K^+ channels have been described (DeCoursey et al., 1987*a*), the cation selectivity has not been previously studied. In addition to presenting this new information, we also describe more completely the kinetics of activation and deactivation. This analysis is extended in the companion paper (Shapiro and DeCoursey, 1991) to include the effects of permeant ion species on gating kinetics. In most respects, type *l* selectivity and permeation characteristics resemble those of voltage-gated K^+ channels in other cells, including frog node of Ranvier (Hille, 1973), frog muscle (Gay and Stanfield, 1978), snail neuron (Reuter and Stevens, 1980), human T lymphocyte (Cahalan et al., 1985), and squid axon (Wagoner and Oxford, 1987). Considering the similarity of type *l* and g_{f2} channels and several advantages of the lymphocyte preparation over node of Ranvier, *lpr* mouse T lymphocytes may be the ideal preparation in which to study this type of K^+ channel.

Preliminary results have been communicated in abstract form (Shapiro and DeCoursey, 1989; Shapiro, 1990).

METHODS

Recording Techniques

The composition of solutions is given in Table I. Micropipettes were pulled in several stages using a Flaming Brown automatic pipette puller (Sutter Instruments, San Rafael, CA), coated with Sylgard 184 (Dow Corning Corp., Midland, MI) and heat polished. EG-6, KG-12, or 0010 glass obtained from Garner Glass Co. (Claremont, CA), reported to have a low intrinsic noise

(Rae and Levis, 1984), formed tight seals (5-30 GΩ) with lymphocyte membranes. Pipette tip resistances measured in Ringer solution ranged between 2 and 5 MΩ. Electrical contact with the pipette solution was achieved by a small sintered Ag-AgCl pellet (In Vivo Metric Systems, Healdsburg, CA) attached to a silver wire covered by a Teflon tube. Pipette and initial bath solutions were filtered at 0.2 μm (Millipore Corp., Bedford, MA). A reference electrode made from a Ag-AgCl pellet was connected to the bath through an agar bridge saturated with Ringer solution. The current signal from the patch clamp (Axopatch-1B, modified to be a 1C; Axon Instruments, Burlingame, CA) was recorded and analyzed using an Indec Laboratory Data Acquisition and Display System (Indec Corp., Sunnyvale, CA). Cells were visualized with a modified Nikon Labophot (Fryer Instruments, Carpentersville, IL), equipped with Hoffmann contrast optics.

TABLE I

Solutions

	Extracellular (bath) solutions					
Name	Na^+	K^+	Ca^{2+}	Mg^{2+}	Cl^-	HEPES
			mM			
Ringer	160	4.5	2	1	170.5	10
K-Ringer	0	160	2	1	170.5	10
X*-Ringer	0	0	2	1	170.5	10

*Rb^+, Cs^+, NH_4^+, Na^+, Li^+, and TMA^+ Ringer solutions were identical to K-Ringer solution with all the K^+ replaced by the chloride salt of the appropriate cation. Solutions were titrated to pH 7.4 with the hydroxide of the predominant cation or with tetramethylammonium hydroxide (TMAOH) for Rb-Ringer solution and Rb^+ mixtures. Hepes is [4-(2-hydroxyethyl)-1-piperazineethane-sulfonic acid].

	Intracellular (pipette) solutions							
Name	K^+	Cl^-	F^-	$CH_3SO_3^-$	Mg^{2+}	Ca^{2+}	EGTA	HEPES
				mM				
KCH_3SO_3	162	6	0	140	2	1	10	10
KF/Cl	162	76	70	0	2	1	11	10
KCH_3SO_3/F	162	6	40	100	2	1	10	10
RbF/Cl*	0	80	80	0	0	0	0	5
CsF/Cl‡	0	80	80	0	0	0	0	5

Solutions were titrated to pH 7.2 with the hydroxide of the permeant cation or with TMAOH for the Rb^+ solution. EGTA is ethylene glycol bis-(β-aminoethyl ether) N,N,N′,N′-tetraacetic acid. Estimated free Ca^{2+} concentration is <43 nM for all solutions, and free Mg^{2+} concentration is <50 nM for fluoride-containing solutions, and 1.9 mM for KCH_3SO_3.
*Plus 160 mM Rb^+ ‡Plus 160 mM Cs^+.

A Klinger system manipulator (Klinger Instruments, Richmond Hill, NY) with a DC stepping motor attached was used for fine positioning of patch electrodes. Lymphocytes did not adhere to the bottom of the glass recording chamber; seals were made by bringing the pipette close to a cell and then quickly turning on the suction, sucking the cell onto the pipette tip. A typical suction pressure used to form seals was −5 inches of water. In general, seals were easy to make using this technique. To achieve whole-cell configuration (Hamill et al., 1981), strong suction was applied to the pipette. Lymphocyte input resistances were very high, typically 20 GΩ or more, in the whole-cell configuration at the holding potential, V_{hold} = −80 mV. Often, the whole-cell input resistance was greater than the pipette seal resistance. Upon seal formation,

the pipette capacity was cancelled with the Axopatch circuitry; after breaking into the cell, the whole-cell capacity transient (typically ~0.7 pF) was nulled. The series resistance read from the dial was usually 2–6 MΩ and was fairly stable throughout the course of the experiment. Series resistance compensation with the Axopatch 1 series clamp can sometimes be problematical and was used only if very large currents were encountered, e.g., with 160 mM K-Ringer solution in the bath.

Most experiments were done at room temperature (19–26°C), with the bath temperature monitored continuously by a thinfilm platinum RTD (resistance temperature detector) element (Omega Engineering, Stamford, CT), and the temperature was stored along with each data run. In some early experiments the room temperature alone was recorded, and the bath temperature was assumed to be 3°C cooler, reflecting measured evaporative heat loss from the bath. A few experiments were done at lower temperatures (8–15°C), with the bath temperature controlled by feedback with Peltier devices (Teca, Chicago, IL).

Data were recorded and analyzed using the *SAP/ANAL* family of programs written by Dr. Richard S. Lewis (Stanford University, CA), in the BASIC-23 language developed for the Indec computer system. Leak and capacity subtraction was accomplished in *SAP* using a P/*n* subthreshold protocol where *m* pulses 1/*n* the amplitude of the test pulses are applied immediately before the test pulse, where *m* and *n* are user-controlled; the leak pulses are averaged, scaled up, and subtracted from the test pulse, thereby allowing the linear leak and residual capacity to be subtracted from the data records.

Most chemicals were purchased from Sigma Chemical Co. (St. Louis, MO) or Aldrich Chemical Co. (Milwaukee, WI). Sigma Chemical Co. has determined that their CsCl contains $<0.01\%$ K^+ or Na^+ as contaminants, so 160 mM Cs-Ringer solution contains <16 μM K^+. Crude *Leiurus quinquestriatus hebraeus* scorpion venom was purchased from Sigma Chemical Co.

Junction Potentials

Data were recorded with a correction for the junction potential that arises when there is an interface between dissimilar salt solutions. Junction potentials arising (*a*) between the pipette solution and the bath solution and (*b*) between the bath (reference) electrode and the bath solution were calculated using the Henderson equation (1907), assuming linear mixing of solutions at the interface. Mobilities were taken from Robinson and Stokes (1965), or derived from equivalent ionic conductances extrapolated to infinite dilution (Vanýsek, 1987). Electrode drift during long experiments was checked by measuring the reversal potential periodically in a standard solution (usually Ringer or K-Ringer solution; reversal potentials were measured after all solution changes) and by breaking the pipette tip at the end of an experiment. When significant drift was detected (i.e., >5 mV), potentials were corrected according to the nearest time point.

Cells

MRL/MpJ-*lpr/lpr* mice were purchased from Jackson Laboratory (Bar Harbor, ME). The greatly enlarged lymph nodes were isolated from mice killed by cervical dislocation. A few experiments were done on spleen cells. Cells were separated by rubbing the nodes between two frosted glass slides and then filtering the suspension through a coarse nylon mesh. Cells were incubated in RPMI media (Hazelton Biologicals, St. Lenexa, KS), with added 10% FCS (Gibco Laboratories, Grand Island, NY), 2 mM glutamine, 1% penicillin/streptomycin, and incubated in 5% CO_2 at 37°C. The pH of the media was adjusted immediately before use with HCl. A fraction of the isolated cells was frozen for future use in a 20% FCS, 5% DMSO freezing medium and stored either in liquid N_2 or in a freezer at −80°C. Some of the data presented here were from thawed cells; type *l* currents in these cells were indistinguishable from those in freshly isolated

lymphocytes. A few experiments included here were done on the human B cell lymphocytic *Loucke*s cell line (generously provided by Drs. D. Wang and E. Kieff, Harvard University, Boston, MA).

RESULTS

The majority of lymphocytes studied from diseased *lpr* mice had large numbers of type *l* K^+ channels. The average saturating chord conductance in Ringer solution (Table I) was 4.9 ± 3.2 nS (mean ± SD, $n = 41$) and 11.2 ± 7.2 nS ($n = 34$) in 160 mM K-Ringer solution. This K conductance, g_K, corresponds to on the order of 300 type *l* K^+ channels in a cell with an input capacity of only 0.7 pF. The g_K is much greater than that of normal murine lymphocytes, but typical of the large type *l* g_K in T cells from mice with the *lpr* mutation (Chandy et al., 1986; DeCoursey et al., 1987*a*; Grissmer et al., 1988). Some lymphocytes displayed only small type *n* currents, with peak K^+ currents corresponding to ~10 channels per cell. Many of the cells with type *l* currents also displayed type *n* currents, of approximately the same magnitude as cells with only type *n* currents. The two types of K^+ currents can be unambiguously identified by tail current kinetics as well as by several other characteristics (DeCoursey et al., 1987*a*); in all cells included in this study both tail current kinetics and a test for accumulation of inactivation during rapid depolarizing pulse trains were used to confirm the identity of the channel type.

Fig. 1 *A* shows a family of typical type *l* currents with KCH_3SO_3 in the pipette and Ringer solution in the bath, recorded during 200-ms depolarizations to potentials from −50 to +60 mV. In this experiment and in all other data obtained in the whole-cell configuration except where indicated, K^+ was the only intracellular monovalent cation. Current–voltage (Fig. 1 *B*) and conductance–voltage curves (Fig. 1 *C*) from this experiment illustrate that type *l* currents are activated by depolarization, first turning on at approximately −20 mV, with half-activation near 0 mV under these conditions.

In Fig. 2, analogous families of currents are shown for cells wherein the only external monovalent cation was K^+, Rb^+, NH_4^+, or Cs^+ (Fig. 2, *A–D*, respectively). It should be noted that all upward currents are outward and are thus carried by the K^+ in the cell; only the inward currents in K^+ and Rb^+ negative to the reversal potential, V_{rev}, are carried by the extracellular permeant ion, as are the inward tail currents in all four solutions when the cell is repolarized to the holding potential of −80 mV. It is apparent in this figure that tail currents in K^+ and NH_4^+ are fast, those in Rb^+ are much slower, and tails in Cs^+ are slow and very small in amplitude. A full treatment of the effect of permeating ion species on deactivation kinetics of type *l* currents is presented in the companion paper (Shapiro and DeCoursey, 1991).

Separation of Type l and Type n K^+ Currents

Most cells displayed tail currents that had a small slow component as well as a large fast component. We interpret these slower components as reflecting the presence in these cells of some type *n* channels, which close slowly, in addition to the dominant type *l* channels, which close 10 times more quickly. Currents from a cell with an exceptionally large type *n* component are shown in Fig. 3 *A*. A short depolarizing

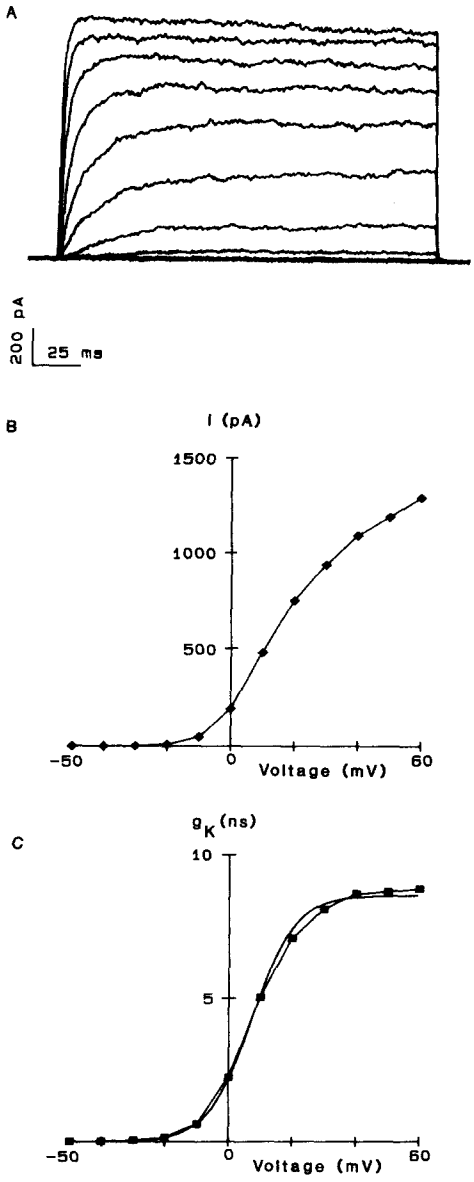

FIGURE 1. Typical family of type *l* currents in a lymphocyte with KCH_3SO_3 in the pipette and Ringer solution in the bath. (*A*) Superimposed are currents recorded during 200-ms depolarizing pulses applied from V_{hold} = −80 mV to potentials from −50 through 60 mV in 10-mV increments. (*B*) Peak current-voltage relationship in the same experiment. (*C*) Peak chord conductance-voltage curve assuming V_{rev} = −85 mV. The smooth curve is a least squares Boltzmann fit given by: g_K (nS) = 8.66/[1 + exp [(7.4-V)/6.86]] (*V* in mV). Input capacity of the cell was 0.7 pF, input resistance was 25 GΩ at V_{hold}, 1 s between pulses, P/4 leak subtraction, no series resistance compensation used, sample interval (*I*) = 458 μs, filter = 500 Hz, 2.1 min after establishing whole-cell configuration. Cell No. 29.

pre-pulse was applied to maximally open K^+ channels and then the cell was repolarized to the holding potential where channel closing can be observed as a "tail" current. Traces are shown before and after the addition to the bath of 278 μg/ml *Leiurus quinquestriatus hebraeus* scorpion venom, which contains the potent K^+ channel blocker charybdotoxin. Type *n*, but not type *l* channels, are blocked by charybdotoxin (Sands et al., 1989); the unpurified venom is also very effective at separating the two channel types. The presence of type *n* channels was detected also by a "shoulder" in the *g-V* curve ~30 mV negative to the larger type *l* component. In Fig. 3 *B*, *g-V*

curves from the same cell as in Fig. 3 *A* are superimposed before and after addition of venom. The amplitude of the slow component in the tail current roughly correlates with the size of the shoulder in the *g-V* relation. *Leiurus* venom at 10 μg/ml was found to be sufficient to completely abolish the type *n* component. This concentration of

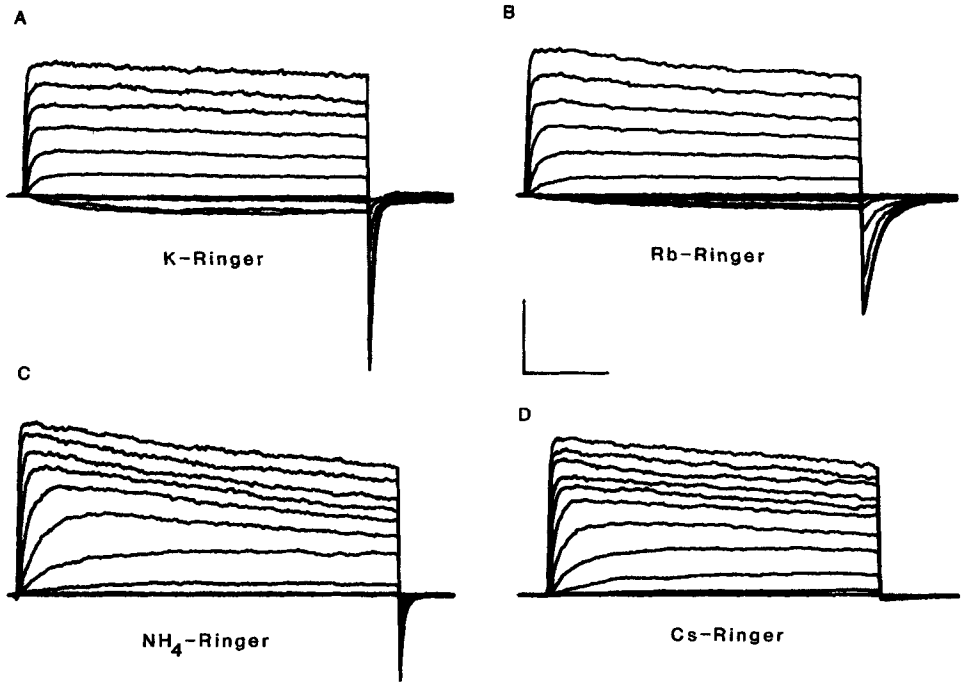

FIGURE 2. Current families with different permeant ions in the bath and K^+ in the cell. All currents recorded during 200-ms depolarizing pulses from V_{hold} = −80 mV to test potentials in 10 mV increments up to 60 mV, with 1–2 s between pulses. Note the characteristic "tail currents" at the end of the test pulses produced when the membrane is repolarized. (*A*) 160 mM K-Ringer solution in the bath. Calibration bars: 48 ms, 400 pA. Pulses start at −40 mV, pipette KCH_3SO_3, filter 1 kHz, 18 min into whole-cell. (*B*) 160 mM Rb-Ringer solution in the bath. Calibration bars: 50 ms, 640 pA. Pulses start at −80 mV, pipette KCH_3SO_3/F, filter 1 kHz, 17 min into whole-cell. (*C*) 160 mM NH_4-Ringer solution in the bath. Calibration bars: 43 ms, 800 pA. Pulses start at −50 mV, pipette KCH_3SO_3, filter 1 kHz, 13 min into whole-cell. (*D*) 160 mM Cs-Ringer solution in the bath. Same cell as in *A*. Calibration bars: 50 ms, 400 pA. Pulses start at −50 mV, filter 500 Hz, 25 min into whole-cell. Series resistance compensation is 80% in *B* and *C* and 0% in *A* and *D*. Input resistances at V_{hold} were 9–25 GΩ. (*A*, *D*) Cell No. 29; (*B*) cell No. 78; (*C*) cell No. 57.

venom was added to solutions in some later experiments, but when added to the pipette solution seals were not obtained.

Open-Channel Rectification and Selectivity

Macroscopic. Instantaneous current-voltage relations (*I-V*s) were obtained with K^+ in the cell under whole-cell voltage clamp for each of the four permeant ions by

applying a prepulse to a potential at which the channels opened maximally (typically 40 mV) and then stepping to various test potentials, as shown schematically in Fig. 4 *D*. At negative test potentials where the channels close, the deactivation (tail) transient fit by eye to a single exponential was extrapolated back to zero time; at positive potentials, the current at the start of the test pulse was recorded. These *I-V*s presumably reflect single channel rectification in the presence of each bathing ion. Instantaneous *I-V*s are shown in Fig. 4 *A* for a cell with Ringer solution in the bath, and then when the bath was changed to K-Ringer or Rb-Ringer solution. The *I-V* in Ringer solution is gently concave over the range of −120 to 50 mV and reverses at

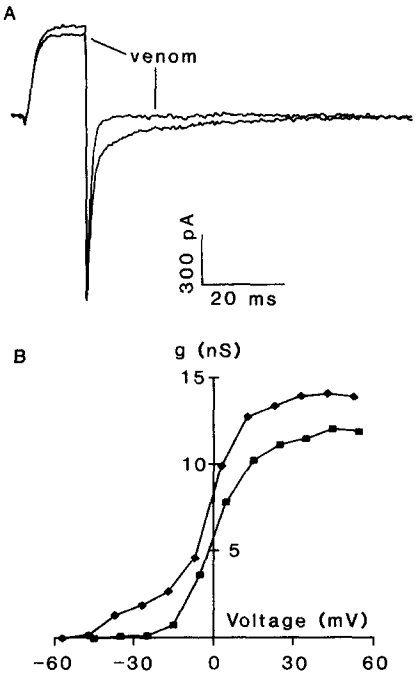

FIGURE 3. (*A*) Block of type *n* component of K^+ current by *Leiurus quinquestriatus hebraeus* venom. Whole-cell currents recorded during a 15-ms pre-pulse to 33 mV to maximally open channels and after repolarization to −87 mV where channel closing is observed. This cell has significant numbers of both type *l* and type *n* channels. The addition of 278 μg/ml *Leiurus* venom to the bath blocks the slowly deactivating type *n* component, leaving the fast-closing type *l* channels unaffected. The fitted time constant (τ_{tail}) after addition of venom is 1.0 ms; the tail before venom was fit by a double exponential with fast component τ of 1.0 ms and slow component τ of 14.8 ms. Cell No. 143. (*B*) Elimination of the type *n* "shoulder" in the *g-V* relation by *Leiurus* venom. Curves are shown before (◆) and after (■) addition of venom. The type *n* component produces a shoulder in the curve around −30 mV. The "after" curve has been corrected by −12 mV due to an observed intrinsic voltage shift of the type *l* voltage dependence with time in whole-cell perfusion (see companion paper, Fig. 1).

−88 mV, near E_K. In symmetrical K^+, the *I-V* displays strong inward rectification, resulting in large inward currents at negative potentials. In cells studied under this condition, the slope conductance was typically about twice as large at negative than at positive potentials. With Rb^+ in the bath the *I-V* displays little rectification and reverses a few mV negative to V_{rev} in K-Ringer solution, indicating that P_{Rb} (0.76, Table II) is only slightly lower than P_K.

In Fig. 4 *B*, *I-V*s are shown for a cell first in K-Ringer solution and then in NH_4-Ringer solution. The shape of the *I-V* for NH_4^+ is strikingly different from that in K^+. In NH_4^+, the *I-V* displays strong inward rectification around V_{rev}, but the slope conductance decreases at more negative potentials. The slope conductance at V_{rev}

−30 mV is one and a half times greater for NH_4^+ than for K^+, even though the reversal potential of −55 mV in NH_4-Ringer solution indicates that NH_4^+ has a relative permeability only one-eighth that of K^+ (Table II). In other words, the relative permeability and relative conductance for NH_4^+ are very dissimilar.

Instantaneous *I-V*s in another cell are shown in Fig. 4 *C*, with Ringer, K-Ringer and Cs-Ringer solutions sequentially in the bath. Profound inward rectification in K-Ringer solution is especially evident in this cell, although the precise amplitude of

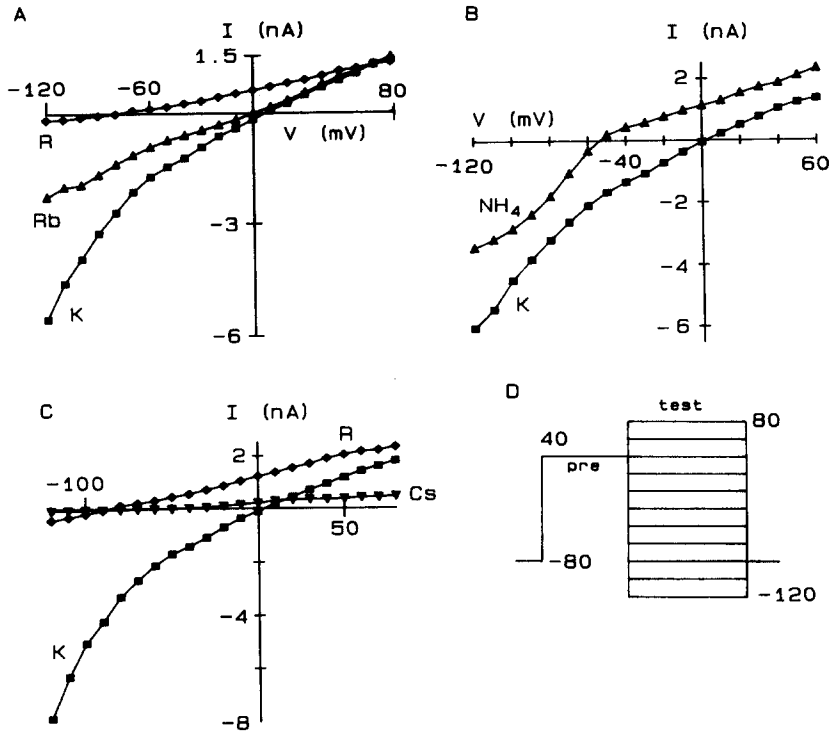

FIGURE 4. Instantaneous current-voltage relations for different external permeant ions. (*A*) Ringer (◆), K-Ringer (■), and Rb-Ringer solution (▲). (*B*) K-Ringer (■) and NH_4-Ringer solution (▲). (*C*) K-Ringer (■), Ringer (◆), and Cs-Ringer solution (▼). (*D*) Protocol used to obtain instantaneous current-voltage relations: a brief pre-pulse is applied to 40 mV to maximally open channels and then a test pulse is applied to the indicated range of potentials. All data are corrected for junction potentials and currents are leak-subtracted, as described in Methods. (*A*) Cell No. 140, (*B*) 57, (*C*) 111.

the current at strongly negative potentials is somewhat approximate because of the dependence on exact series resistance compensation necessitated by the large magnitude of the current. In Cs-Ringer solution, V_{rev} is −55 mV, the same as that in NH_4^+, so by this criterion these ions have the same relative permeability (Table II); however, inward Cs^+ currents are very small. Even when the *I-V* in Cs^+ is scaled up so that the outward currents are the same, the relative conductance for Cs^+ ions is only a small fraction of that for NH_4^+. Evidence that the inward currents in Cs-Ringer

solution are type *l* currents includes their block by 2 mM TEA^+ and the lack of any other inward conductance in *lpr* lymphocytes (e.g., Na^+ or Ca^{2+} currents). Contamination of Cs^+ by trace K^+ is too low to account for the observed currents (see Methods).

After replacement of all bathing K^+ with Cs^+, both inward and outward currents are greatly reduced (▼, Fig. 4 *C*). The reduction of outward currents is much greater than that predicted by the Goldman-Hodgkin-Katz current equation. In other experiments, washout of Cs-Ringer with Ringer or K-Ringer solution only partially restored the current. Apparently Cs-Ringer solution in the bath does not simply block the current but rather irreversibly reduces the number of functioning channels. This interpretation is supported by single channel measurements in the on-cell patch

TABLE II

Relative Permeabilities and Conductances (Whole-Cell, K^+ in the Cell)

Ion	P_{rel}	g_{rel}	N
K^+	≡1.0	≡1.0	–
Rb^+	0.76	0.5	7
NH_4^+	0.12	1.5	5
Cs^+	0.12	<0.06*	6
Na^+	<0.005	Undefined	2

Relative permeabilities, P_{rel}, were calculated from reversal potentials V_{rev}, with K^+ as the monovalent cation in the intracellular (pipette) solution under whole-cell clamp and the Ringer of the indicated ion in the bath. From V_{rev} in bi-ionic conditions, the permeability relative to that of K^+ was calculated using the Goldman-Hodgkin-Katz equation: $V_{rev} = RT/zF \ln([A]_o P_A/[B]_i P_B)$, where $[A]_o$ and $[B]_i$ are the concentrations of the external and internal permeant ions, respectively, P_A and P_B are the permeabilities, R is the gas constant, T is the temperature (°K), z is the valence, which is one, and F is Faraday's constant. For the case of internal K^+, P_A/P_B is the relative permeability. Relative conductances, g_{rel}, are the slope conductances measured 30 mV negative to the reversal potential. This measurement of conductance was chosen to reflect the ability of the external permeant ion to carry current. Since the *I-V* for each ion rectifies differently, measuring g_{rel} at another potential would result in somewhat different values.

*Because currents were irreversibly diminished in Cs-Ringer (see text), g_{Cs} was estimated by scaling the inward Cs^+ currents by the ratio of outward currents in Ringer before and after the Cs^+ measurement.

configuration, in which outward currents carried by K^+ from the cell with Cs^+ in the pipette were as large as when K^+-containing pipette solutions were used (Fig. 5, compare *A* and *C*). Profound rundown was also seen with K-free Na-Ringer solution (data not shown), but not with the other three permeant ions studied. Perhaps type *l* channels need external permeant ions to remain functional, a need only partially satisfied by 160 mM Cs^+. Analogous phenomena occur in squid delayed rectifier (Chandler and Meves, 1970; Almers and Armstrong, 1980).

Table II summarizes the selectivity data for experiments with K^+ in the cell. The sequence of relative permeability calculated from V_{rev} measured under bi-ionic conditions using the Goldman-Hodgkin-Katz equation is K^+ (≡1.0) > Rb^+ (0.76) > NH_4^+, Cs^+ (0.12) ≫ Na^+, Li^+ (<0.005). The conductance sequence measured at V_{rev}

-30 mV is different: NH_4^+ (1.5) > K^+ ($\equiv$1.0) > Rb^+ (0.5) > Cs^+ (0.06) $\gg$ Na^+. Relative permeabilities and conductances are often different, but NH_4^+ seems anomalous with g_{NH_4} at least 10 times *greater* than P_{NH_4} (both relative to K^+), while the relative conductances of Rb^+ and Cs^+ are *lower* than their respective relative permeabilities.

It is of interest to know whether ionic permeability is the same regardless of the side of the membrane on which the ion is present. In one cell of those studied with RbF/Cl in the pipette (and thus Rb^+ as the intracellular permeant ion), P_{Rb} was 0.82, similar to P_{Rb} measured with Rb-Ringer solution in the bath. The *I-V* in symmetrical

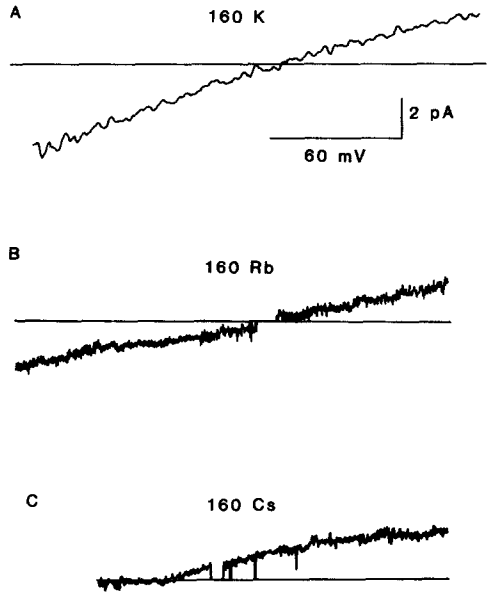

FIGURE 5. Single-channel current-voltage (*i-V*) relationships in on-cell patches with K^+, Rb^+, or Cs^+ in the pipette. Ensemble average leak-subtracted open-channel currents during voltage ramps, with K-Ringer solution in the bath in all cases. (*A*) KCH_3SO_3/F in the pipette. Ramp from RP +120 mV to RP -87 mV. Ramp speed 16 mV/ms, filter 2 kHz. The ramp speed was much faster in *A* because channels close much faster with K^+ than with Rb^+ as the external permeant ion. The resting potential (RP) of the cell, estimated by assuming that V_{rev} is 0 mV, was -27 mV. Cell No. 138. (*B*) RbF/Cl in the pipette. For technical reasons, it was not possible in this experiment to record the entire open-channel *i-V* by ramping down. Therefore, the *i-V* from RP -35 mV to RP -120 mV was obtained by ramping down, and that from RP -40 mV to RP +80 mV by ramping up, and the two segments joined to reconstruct the entire range. Up-ramp: ramp speed 0.53 mV/ms, filter 1 kHz, resting potential estimated to be -4 mV. Down-ramp: ramp speed 0.75 mV/ms, filter 1 kHz, cell No. 146. (*C*) $CsCH_3SO_3$ in the pipette. It could not be determined whether the channel was open or closed at potentials negative to the apparent reversal potential. Ramps from RP +80 mV to RP -80 mV at 0.68 mV/ms, filter 500 Hz, cell No. 94.

Rb^+ was approximately linear (data not shown). Most of the successful experiments with Cs^+ in the pipette were done with the human B cell *Loucks* cell line, which also have type *l* K^+ channels (Shapiro and DeCoursey, 1988). P_{Cs} estimated from V_{rev} in *Loucks* cells with Cs^+ internally and K^+ externally was 0.13, indistinguishable from P_{Cs} with K^+ internally and Cs^+ externally. In cells studied with NH_4^+ in the pipette, seals were poor, and large leak currents in the whole-cell configuration precluded good estimates of V_{rev}. In summary, under the conditions studied, permeability ratios appear to be independent of which side of the membrane the ions were present.

Microscopic. We investigated the single open channel current-voltage relation (*i-V*) in on-cell patches with K^+, Rb^+, or Cs^+ in the pipette. Currents were recorded during voltage ramps from positive to negative potentials. Type *l* channels typically are open at the start of the ramp and stay open for a variable time before closing as the ramp potential goes negative. We used only on-cell data where the resting potential appeared to be fairly steady; the bath solution used in these experiments was K-Ringer in order to "clamp" the resting potential near 0 mV. Fig. 5 shows average leak-subtracted *i-V*s assembled from many ramps, with 160 mM K^+, 160 mM Rb^+, or 160 mM Cs^+ in the pipette (Figs. 5, *A–C,* respectively). A much faster ramp rate was used for measurements with K^+ in the pipette than with Rb^+ or Cs^+ since the channel closes much faster with K^+ as the external permeant ion (Fig. 2 and companion paper). With high K^+ concentrations on both sides of the membrane the channel rectifies inwardly, with a slope conductance of ~36 pS at −100 mV, decreasing to ~23 pS at 60 mV. When the pipette contained Rb^+, the *i-V* exhibited little rectification, with a slope conductance of ~15 pS at negative potentials (where Rb^+ is the charge carrier) and ~18 pS at positive potentials. Thus with K^+ or Rb^+ in the pipette, single channel rectification resembles that of the macroscopic instantaneous *I-V* relation in K-Ringer or Rb-Ringer solutions, respectively. For inward currents at negative potentials the Rb^+ conductance, g_{Rb}, is slightly less than half of g_K, again comparable to g_{Rb}/g_K estimated from macroscopic *I-V* measurements. The outward current with Cs^+ in the pipette (Fig. 5 *C*) at large positive potentials is as large as the outward current at comparable potentials with K^+ in the pipette. Evidently, Cs^+ in the external solution does not interfere with K^+ efflux through type *l* channels. No inward Cs^+ current could be resolved at the single channel level. Scaled from the macroscopic *I-V* in Cs-Ringer solution, single channel inward Cs^+ current at −100 mV would be 0.05 pA, well below the resolution of our measurements.

Mole-fraction dependent permeabilities. Multi-ion channels may exhibit anomalous mole fraction effects (e.g., Hille and Schwarz, 1978). We studied the mole fraction dependence of the NH_4^+ permeability in K^+-NH_4^+ mixtures because both ions carry large currents, and the reversal potentials in isotonic K^+ or NH_4^+ differ by a large amount. Fig. 6 summarizes the results. The permeability ratio P_{NH_4}/P_K is 0.12 ± 0.02 (mean ± SD in four cells) in 160 mM NH_4-Ringer solution, but falls to a value less than half that in 20 K^+, 140 NH_4^+, 0.032 ± 0.019 ($n = 3$), which is significantly smaller ($P < 0.005$). As the fractional K^+ concentration is increased further, P_{NH_4}/P_K increases again, although at the high K^+ end the absolute size of changes in V_{rev} becomes small and hard to quantify. There is thus a minimum in the permeability ratio for NH_4^+-K^+ mixtures. We found no obvious minimum in the relation between mole fraction and conductance, however. Some measurements were made in K^+-Rb^+ mixtures, but because of the small total range of V_{rev} encompassed by a complete change from K-Ringer to Rb-Ringer solution, we could not determine whether P_{Rb} varies with mole fraction.

Type l Kinetics: Macroscopic

Activation kinetics. Type *l* current activation could not be fit by traditional Hodgkin-Huxley (1952) n^4 kinetics, unlike type *n* currents in lymphocytes (Cahalan et al.,

1985), and in fact was poorly fit by any one order of exponential over the entire voltage range studied, consistent with earlier work (DeCoursey et al., 1987*a*). Activation was well fitted, however, at all potentials by a variable short delay followed by a single exponential, as illustrated in the right inset in Fig. 7. The time constants of these single exponentials are the τ_{act} data plotted in Fig. 7. The rate of activation was voltage dependent, with τ_{act} decreasing *e*-fold in ~20 mV between the peak and 60 mV more positive (*filled symbols*), with an increasingly gradual decrease in τ_{act} at more positive potentials, and apparently approaching a limiting value at >100 mV positive to the half-activation potential.

The delays needed to fit the rising phase of type *l* currents were also voltage dependent, becoming shorter with increasing depolarization. Delays were somewhat less precisely defined by the data, but their voltage dependence could be generally

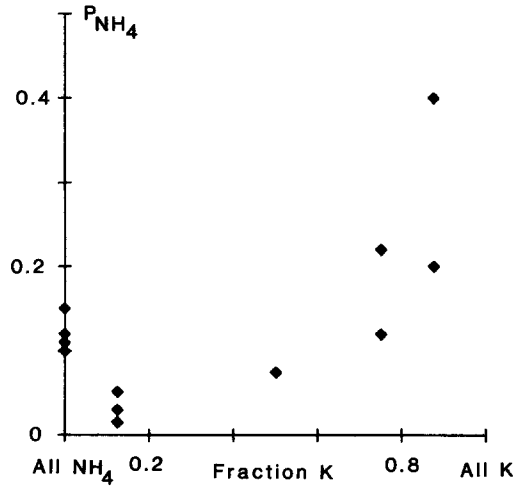

FIGURE 6. Dependence of the NH_4^+ permeability on mole fraction in K^+-NH_4^+ mixtures. Instantaneous *I-V* curves were obtained with different isotonic K^+-NH_4^+ mixtures in the bath and 160 mM K^+ in the cell. Plotted are the permeabilities for NH_4^+ relative to K^+ as a function of mole fraction of K^+ in the solution, calculated using the Goldman-Hodgkin-Katz equation for the measured V_{rev} for each experiment. Only cells in which V_{rev} was also measured in K-Ringer solution as reference were included. Each point represents a different measurement, with a total of eight cells.

described as exponential, decreasing *e*-fold for ~75 mV depolarization. Since the voltage dependence of the delay is less steep than that of τ_{act}, especially for moderate depolarizations, the ratio of the delay to τ_{act} increases with depolarization.

Deactivation kinetics. We quantified the deactivation kinetics of type *l* currents by fitting tail currents to an exponential curve by eye. The left inset of Fig. 7 illustrates an outward tail current (*dotted curve*) recorded in Ringer solution at −40 mV with a fitted single exponential (*solid curve*). Most tail currents were fit well with a single exponential if adequate series resistance compensation had been used. In cells in which there was a significant fraction of type *n* (slow-closing) channels, a double exponential curve was fit to the tail currents, with the faster component corresponding to the type *l* channels, as was demonstrated in Fig. 3. The deactivation time constant, τ_{tail}, for type *l* currents was voltage dependent, decreasing monotonically at more negative potentials (*half-filled symbols*, Fig. 7). The voltage dependence was

steepest between −20 and −70 mV, changing *e*-fold in ~25 mV and became more gradual at strongly negative potentials. The τ-V curve is approximately bell-shaped.

The voltage dependence of type *l* channel gating was not constant but shifted with time after achieving whole-cell configuration. The two sets of deactivation and activation time constants in Fig. 7 were obtained at different times after achieving whole-cell configuration in Ringer solution. In this experiment, both activation and deactivation time constants shifted to the left, although τ_{act} seems somewhat more profoundly shifted. In cells subjected to this analysis, many displayed voltage shifts in

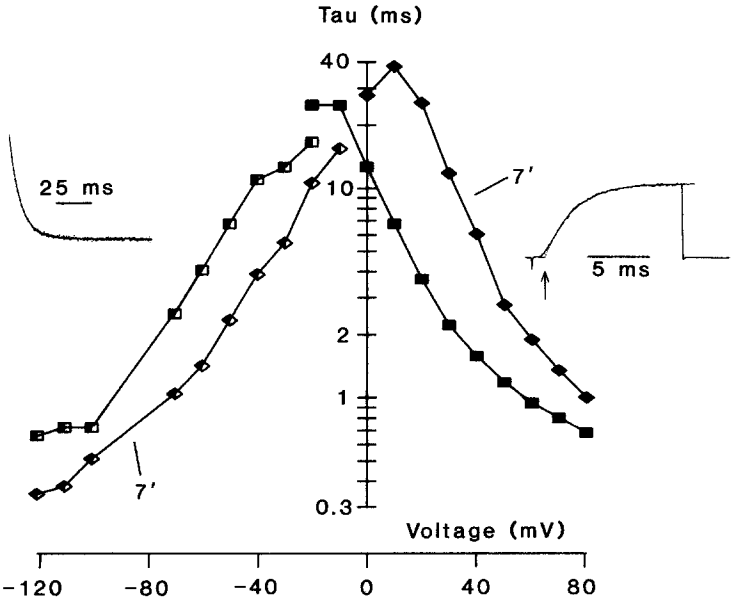

FIGURE 7. Voltage-dependence of activation (*filled symbols*) and deactivation (*half-filled*) time constants at 7 (◆) and 40 (■) min in whole-cell. Activation time constants were fit to a single exponential after a short delay, as illustrated in the right inset. Superimposed in the right inset are a current record from a 12-ms pulse to +60 mV (*solid curve*) and the fitted curve (*dotted line;* τ_{act} = 2.25 ms, delay = 1.1 ms, amplitude = 1,392 pA). The "delay" in this fit is the interval from the capacity blip, indicating the start of the pulse, up to the arrow. Activation kinetics at all potentials were well fit using this approach. In the left inset are superimposed a current record from the tail pulse to −40 mV (*dots*) and the exponential fit (*solid curve;* I_{peak} 425 pA, τ 3.8 ms). Pipette KCH_3SO_3/F, bath Ringer solution, filter 5 kHz, 19–20°C, cell No. 78.

both activation and deactivation, with activation shifts somewhat more pronounced, while in others, τ_{tail} was not detectably shifted. This spontaneous shift in the voltage dependence of gating is explored in more detail in the Methods of the companion paper (Shapiro and DeCoursey, 1991).

Hooks. Inward tail currents in Cs-Ringer and Rb-Ringer solution displayed "hooks," i.e., the tail current first increased or remained constant before decaying exponentially. The early part of the tail currents at several potentials is illustrated for a cell in Rb-Ringer solution in Fig. 8 *A* and another cell in Cs-Ringer solution in Fig.

8 *B*. The hooks are especially pronounced in Cs-Ringer solution, in which the current distinctly increases before decaying exponentially. In Rb-Ringer solution the hook usually appears as a delay or flat part before the exponential decline of the current. At lower temperatures (8–10°C) hooks in Rb^+ also had a distinct rising phase. Hooked tail currents in both Cs^+ and Rb^+ were well fit by the sum of two exponentials, one rising and one falling (data not shown). The hooks are not due to a capacitance artifact or the result of contamination by another conductance since: (*a*) hooks were seen in experiments in which there was no evidence of a series resistance problem (i.e., the tail currents in K-Ringer solution, which are larger than those in Rb-Ringer solution, decayed monoexponentially; hooks were most pronounced in Cs-Ringer solution in which currents were smallest and therefore least likely to have series resistance problems); (*b*) hooked tail currents in Cs-Ringer solution were abolished when 2 mM TEA was added to the bath (data not shown); (*c*)

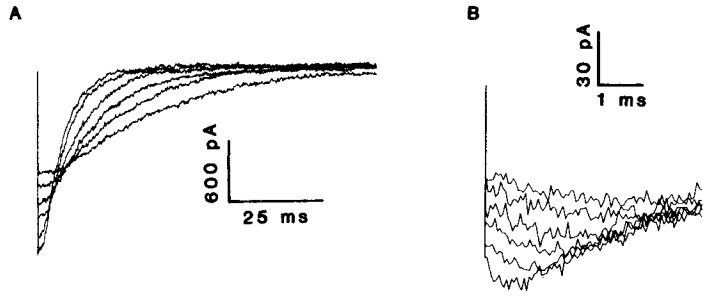

FIGURE 8. Tail currents in Rb^+ and Cs^+ with "hooks" are shown on an expanded time base. (*A*) Tail currents in Rb-Ringer solution from −120 to −70 mV. Hooks are manifested as a delay or flat part of the current in the first 2–8 ms before the exponential relaxation of the currents. The prepulses are not shown. Filter 5 kHz. (*B*) Tail currents in Cs-Ringer solution from −126 to −76 mV. The hooks in the tails here are clearly defined as an initial rise in the amplitude of the current before their exponential relaxation. In addition, the kinetics of the hooks here are clearly voltage dependent. Filter 5 kHz, 18–19°C, 0% SR compensation. (*A*) Cell No. 78; (*B*) cell No. 29.

the time constant of the rising component of the hook was clearly voltage dependent, and, especially at more positive potentials, was slower than the capacity transient, and (*d*) hooks were seen in Rb^+ in experiments done at low temperatures, in which case the relative amplitude and kinetics of the hooks were scaled approximately along with those of the decaying component of tail currents. Hooks were not detected in Ringer, K-Ringer, or NH_4-Ringer solutions. Mechanisms that might give rise to hooks are presented in the Discussion.

Single-channel deactivation. Microscopic closing kinetics were studied in on-cell patches as for the whole-cell currents; i.e., by applying a brief depolarizing prepulse to open channels in the patch and then stepping back to hyperpolarizing potentials where closing is observed. The resting potential was "clamped" near 0 mV by having K-Ringer solution in the bath. Fig. 9 illustrates an experiment with a patch containing several type *l* channels and at least one type *n* channel with a Ca-free, 160

mM K^+ solution in the pipette. We were unable to form tight seals with Ca-containing solutions (such as Ringer or K-Ringer solution). These permeant ionic conditions presumably correspond to the whole-cell case of high K^+ on both sides. Three current records are shown in *A*. In the first two records, two (*top*) or one (*middle*) type *l* channels were open at the end of the prepulse and then quickly closed upon repolarization to −70 mV. Type *l* channels characteristically close quickly and tend to stay closed. For example, in this experiment, out of 72 type *l* events only four distinct reopenings were observed at −70 mV. Since type *l* channels close rapidly anyway upon hyperpolarization, brief reopenings could have been missed. Type *l* events were

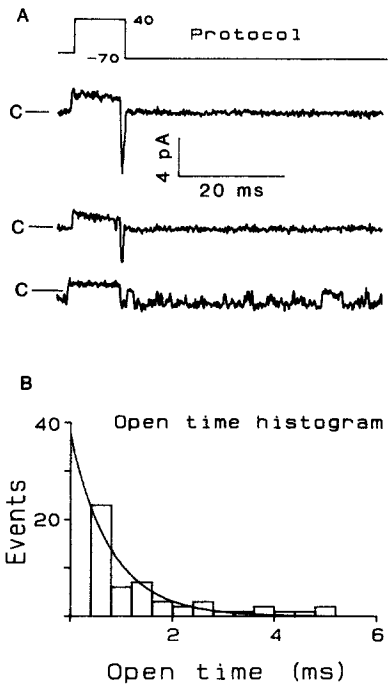

FIGURE 9. Closing of type *l* channels at approximately −70 mV in on-cell patches. (*A*) Shows three records from the 100 recorded in this run, elicited by the pulse protocol shown. Zero current is indicated by the "C" to the left of each trace. Leak and capacity currents averaged from sweeps in which no channels opened have been subtracted from these records. Potentials given are based on the assumption that the cell was depolarized to near 0 mV by K-Ringer solution in the bath. In the first two traces two (*top*) or one (*middle*) type *l* channel was open at the end of the prepulse. An example where only a type *n* channel opened is shown in the bottom trace. Note that it was open already at the start of the trace, before the prepulse. The type *l* open-time histogram for the tail openings is shown in (*B*), fit by least-squares to a single exponential with τ 0.81 ms and amplitude 37.4 events. The first bin was disregarded in the fit and is not shown. Pipette KCH_3SO_3/F, V_{hold} RP-60 mV, filter 2 kHz, I 121 μs, cell No. 140.

distinguished from type *n* events, an example of which is shown in the bottom record, by their greater unitary amplitude and their relatively flicker-free openings. The type *l* open-time histogram from many closing events in Fig. 9 *B* is fit by a single exponential with a time constant, τ, of 0.81 ms.

Ensemble currents from the experiment in Fig. 9 are shown in Fig. 10 *A*,in which only the events interpreted to be type *l* were included. Superimposed on the ensemble trace in *A* is a single exponential fitted by eye, with τ equal to 0.76 ms. The record is very well fit by the line, and the time constant is nearly identical to that fit to the open-time histogram. The ensemble current for all traces from this experiment is

shown in Fig. 10 *B*. The total ensemble in *B* was well-fit by adding a second slower exponential (τ = 7.2 ms) to the fast component, which has a time constant (0.83 ms) similar to that in Fig. 10 *A*. The slower component represents the closing of type *n* channels that occasionally opened during the recordings. The similarity of the type *l* ensemble time constant to the open-time histogram corroborates the observation that type *l* channels rarely reopen after closing. After recording on-cell data from this cell, the patch was ruptured and whole-cell currents were recorded. The cell proved to have large type *l* currents, with only small type *n* currents. Fig. 10 *C* shows a whole-cell tail current to −70 mV, fit with a large fast exponential (τ_{tail} = 0.97 ms) and a small slow component (τ_{tail} = 9.8 ms). The ratio (*l*/*n*) of time constants in whole-cell (0.10) is similar to that seen in the patch (0.11). Thus whole-cell and

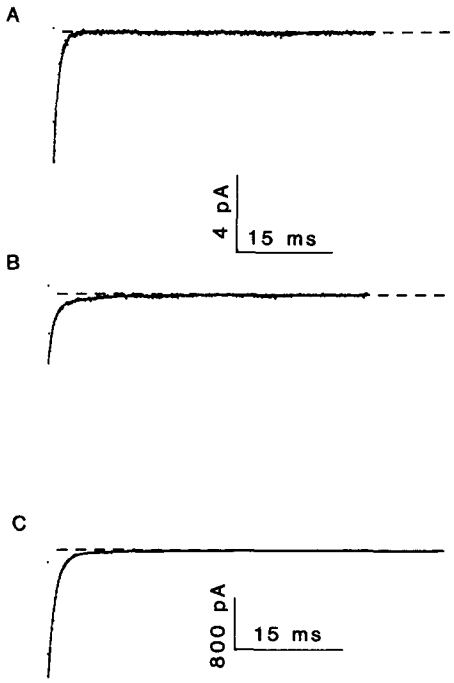

FIGURE 10. Ensemble currents, from the data in Fig. 9, including only events judged to be type *l* (*A*) or all events (*B*). Whole-cell configuration was achieved after acquiring on-cell data; a whole-cell tail current to −70 mV with K-Ringer solution (2 mM Ca^{2+}) in the bath is shown in *C*. Superimposed on the data (*dots*) are exponential curves (*solid lines*) adjusted by eye, fit with one exponential (*A*, τ 0.76 ms), or to a fast plus a slow exponential (*B*, τ_f 0.83 ms, τ_s 7.24 ms; *C*, τ_f 0.97 ms, τ_s 9.8 ms). The fast and slow components are due to the closing of type *l* and type *n* channels, respectively (compare Fig. 3).

single-channel closing kinetics agree; single type *l* channels apparently close in the presence of only a few nanomolar external Ca^{2+}, with kinetics similar to those of tail currents in the whole-cell configuration with 2 mM Ca^{2+} in the bath.

DISCUSSION

Selectivity and Permeation

The relative cation permeability of type *l* channels presented in Table II is similar to that reported previously for delayed rectifier K^+ channels in a variety of preparations (Hille, 1973; Gay and Stanfield, 1978; Coronado et al., 1984; Cahalan et al., 1985; Kawa, 1987; Lucero and Pappone, 1989). These studies report relative permeabilities

of 0.63–0.95 for Rb^+ and 0.10–0.18 for NH_4^+. Type *l* channels appear to differ from other K^+ channels in having a P_{Cs} as large as P_{NH_4}, 0.12, while in most other preparations P_{Cs} is substantially lower.

The relative conductance reported here for Rb^+ (0.5, Table II) is similar to that found in previous work on delayed rectifiers (estimated at V_{rev} −30 mV from their figures) in myelinated nerve: 0.5 (Århem, 1980) and 0.69 (Plant, 1986); and in brown fat cells: 0.47 (Lucero and Pappone, 1989); but somewhat higher than that in squid: 0.25–0.31 (Swenson and Armstrong, 1981; Matteson and Swenson, 1986). In Cs-Ringer solution, small but well-defined inward tail currents carried by Cs^+ through type *l* K^+ channels were seen. Some other delayed rectifier K^+ channels allow weak Cs^+ currents (e.g., Gay and Stanfield, 1978; Cahalan et al., 1985; Hadley and Hume, 1990), while most investigators report negligible Cs^+ permeation (Pickard et al., 1964; Bezanilla and Armstrong, 1972; Hille, 1973; Coronado et al., 1984; Lucero and Pappone, 1989).

The surprisingly high NH_4^+ conductance through type *l* channels (1.5 times g_K at V_{rev} −30 mV), is a value well beyond nearly all previous results on K^+ channels. Interestingly, NH_4^+ was the only one of several dozen monovalent cations tested in endplate channels that had a greater conductance (relative to Na^+) than expected from independence or from permeability ratios (Adams et al., 1981). The decrease in slope conductance of the *I-V* in NH_4^+ at large negative potentials is reminiscent of "self-block" by Tl^+ (Wagoner and Oxford, 1987). We do not know if this is a true property of the single channel *I-V* at this NH_4^+ concentration (160 mM), because we were unable to form seals on lymphocytes with NH_4-containing pipette solutions. It is also conceivable that there is some unusual gating process seen only in NH_4^+, or that external Ca^{2+} blocks only in NH_4-Ringer solution. A speculative interpretation is that the permeation of NH_4^+ (pK_a of NH_4^+ = 9.24) protonates a channel residue in or near the pore (at a site inaccessible to buffer molecules) and so the block at negative potentials in NH_4-Ringer solution is equivalent to proton block of Na^+ channels in low pH solutions (Woodhull, 1973) and in other K^+ channels (Hille, 1968; Drouin and The, 1969). This idea is also consistent with the 15 mV right-shift of the *g-V* curve in NH_4-Ringer solution (companion paper).

The whole-cell instantaneous current-voltage relations (*I-V*s) described in this study are a measure of the ability of the permeant ion present to carry current as a function of voltage. These *I-V*s will precisely reflect relative unitary conductance under different ionic conditions if the same number of channels are open after a large depolarizing prepulse that activates the population of channels maximally. In the general case that the open probability is different for each ion species at maximal activation, the macroscopic *I-V* will accurately reflect single channel rectification but not relative unitary conductance. Since g_{Rb}/g_K of single type *l* channel currents is similar to that obtained from macroscopic *I-V*s, apparently a similar fraction of type *l* channels are open during large depolarizations in K-Ringer and Rb-Ringer solutions, and consequently, the macroscopic *I-V* provides a good estimate of both single channel rectification and g_{Rb}.

Type *l* channels display distinct inward rectification in symmetrical K^+ solutions, while in Rb-Ringer solution the *I-V* is approximately linear with either internal K^+ (Figs. 4 and 5) or Rb^+ (data not shown). In addition, within the accuracy of our data,

type *l* channel permeability ratios for Rb^+ (and Cs^+) appeared to be independent of the side of the membrane to which they were added. These results suggest that the potential energy profile "seen" by K^+ ions during permeation through type *l* channels is less symmetrical than that encountered by Rb^+. The "fast" K^+ conductance (g_f) in frog node of Ranvier (Plant, 1986) rectifies much like type *l* channels in K^+ or Rb^+ solutions, as do type *n* K^+ currents in T lymphocytes (Cahalan et al., 1985), and delayed rectifier K^+ channels in frog skeletal muscle (Spruce et al., 1989). In contrast, in squid axon the *I-V* in symmetrical K^+ solutions is relatively linear but exhibits strong outward rectification with Rb^+ in the bath (Swenson and Armstrong, 1981; Clay and Shlesinger, 1983; Wagoner and Oxford, 1987). Thus K^+ permeation in squid has been modeled using fairly symmetrical energy profiles for K^+, with asymmetrical barriers and/or wells introduced to describe permeation of Rb^+ or other ions (Matteson and Swenson, 1986; Wagoner and Oxford, 1987). Asymmetry of the permeation pathway of squid K^+ channels is also suggested by the finding in squid of a lower relative permeability when Rb^+ or NH_4^+ is applied internally than when applied externally (Wagoner and Oxford, 1987). However, Spruce et al. (1989) and Plant (1986) also report lower P_{Rb} when Rb^+ is applied internally.

The "anomalous" mole fraction dependence of P_{NH_4} in type *l* channels (Fig. 6) closely resembles the anomalous mole fraction dependence of the slope conductance in squid in NH_4^+ and K^+ mixtures (Wagoner and Oxford, 1987), with a clear minimum in both cases at ~10% K^+. Mole fraction–dependent permeability ratios indicate that, like most K^+ channels (Hille and Schwarz, 1978), type *l* channels are multi-ion pores.

The most remarkable violations of independence for type *l* channels are the cases of NH_4^+ and Cs^+ ions, which have an equal permeability but vastly different conductances (Table II). If one thinks of permeability as a measure of how easily an ion enters the channel pore, and conductance as a measure of how rapidly the pore is traversed (Hille, 1975), then once inside, NH_4^+ permeates quickly, whereas Cs^+ gets "stuck" in permeation.

Kinetics. We were unable to fit type *l* currents with Hodgkin-Huxley-type n^4 kinetics, a result consistent with previous studies (DeCoursey et al., 1987*a*). The delay followed by a single-exponential fitting approach we used was arbitrary and certainly real currents do not have a sharp inflection at the end of a delay. However, the subsequent rising phase of type *l* currents was fit remarkably well at all potentials. K^+ currents in node of Ranvier similarly are well-fitted by a delay preceding a single exponential (Dubois, 1981*a*). Depolarization to threshold potentials negative to the midpoint of the *g-V* relation, $V_{1/2}$, elicited currents with faster τ_{act} than at $V_{1/2}$; i.e., τ_{act} and τ_{tail} tended to converge, with a maximum near the midpoint of the *g-V* curve, both in K^+-containing or Rb^+-containing solutions. This suggests that activation (after a delay presumably caused by passage through a series of closed states) and deactivation can be approximated by a first order transition between two states, with half-activation at the peak of the τ-*V* curve.

Tail currents with hooks. Inward tail currents with Rb^+ or Cs^+ in the external solution frequently displayed "hooks." Hooked tail currents classically have been associated with blockade of K^+ channels by internal cationic blockers (e.g., Armstrong, 1975; Shapiro, 1977). However, we observed hooks when the only intracellu-

lar cation was K^+ or Rb^+. Ascribing the hooks to block by a potent hypothetical contaminant would not account for the absence of hooks with K^+ or NH_4^+ in the bath. Apparently then the hooks reflect an intrinsic gating mechanism of type *l* channels. Possibly there is a nonconducting or lower conductance state that a substantial fraction of channels occupy at positive potentials, from which upon repolarization the channels must pass through the open state before closing (a "*trans*-open" state). Given this hypothesis, the transition from the *trans*-open state might become apparent only under ionic conditions (e.g., external Rb^+) that result in profoundly slowed deactivation. Thus, hooks may be present in K-Ringer solution but would be too fast to resolve if scaled the same as the subsequent decaying phase; alternatively, Rb^+ and Cs^+ may reveal a kinetic step that is not detectable until specific deactivation

TABLE III

Type L K^+ Channels vs. G_{f2} K^+ Channels

Characteristic	Type *L*	G_{f2}
g_K midpoint ($V_{1/2}$)	−10 to 0 mV (10, 12)	−20 to 5 mV (5, 6, 7, 8)
τ_{tail} (−90 mV, 20°C)	0.8 ms (10, 12)	~0.8 ms (2, 3, 5, 8)
τ_{act} (30 mV, 20°C)	2 ms (10)	1–2 ms (2, 4)
Activation kinetics:		
n^4 kinetics	No (10, 12)	No (4)
delay + 1-exp	Yes (10)	Yes (4)
τ_{inact} in K-Ringer	~1 s (11, 13)	~1 s (1, 5)
Unitary conductance (inward, high K^+)	~33 pS (10)	30 pS (9)
Rb^+ permeability	$P_{Rb}/P_K = 0.76$ (10)	0.76 (8)
Rb^+ conductance	$g_{Rb}/g_K = 0.5$ (10)	0.5 (8)
Slowing effect of $[Rb^+]_0$ on τ_{tail}	~10-fold (15)	~5-fold (8)
TEA sensitivity, K_D	~80 μM (12)	~150 μM (5)
4-AP sensitivity, K_D	<200 μM (12)	10 μM (5)
Block by capsaicin	Yes, time-dependent (13)	Yes, time-dependent (6)
Block by naloxone	Yes, time-independent (13)	Yes (7)
Block by charybdotoxin	No (10, 14)	?

References: (1) Schwarz and Vogel, 1971; (2) Palti et al., 1976; (3) Ilyin et al., 1980; (4) Dubois, 1981*a*; (5) Dubois, 1981*b*; (6) Dubois, 1982; (7) Hu and Rubly, 1983; (8) Plant, 1986; (9) Jonas et al., 1989; (10) this study; (11) unpublished observations of the authors; (12) DeCoursey et al., 1987*a*; (13) Shapiro, 1990; (14) Sands et al., 1989; (15) Shapiro and DeCoursey, 1991.

steps affected by these ions are slowed. Tail currents with hooks in K^+-containing solutions have been reported in cardiac delayed rectifier, in which they were attributed to rapid removal of depolarization-induced "inactivation" (Shibasaki, 1987).

Previous work on K^+ channels has emphasized the importance of Ca^{2+} ions in channel gating or selectivity. One proposal is that Ca^{2+} or other divalent cations bound externally stabilize the closed conformation of the K^+ channel, dissociating when the channel opens (Gilly and Armstrong, 1982; Armstrong and Matteson, 1986). Another proposal is that K^+ channels close preferentially with a Ca^{2+} ion bound within the pore (Armstrong and Matteson, 1986), and that in the absence of Ca^{2+} gating as well as selectivity reversibly disappear (Armstrong and Lopez-Barneo,

1987). While we did not test the effect of Ca^{2+} ions on selectivity, we discerned no obvious modulatory role of external Ca^{2+} in gating when comparing on-cell patch (nanomolar Ca^{2+}) and whole-cell (2 or 20 mM Ca^{2+}) data. Changing the external [Ca^{2+}] between 2 and 20 mM in whole-cell experiments shifted activation and deactivation time constants about equally by 10–15 mV (data not shown), consistent with shifts explainable by traditional surface charge theory (e.g., Hille, 1968; Gilbert and Ehrenstein, 1969; Mozhayeva and Naumov, 1972). Apparently Ca^{2+} plays a smaller role in type *l* K^+ channel gating than in squid K^+ channels. Lymphocytes did not survive long enough in Ca-free bathing solutions to be studied in whole-cell mode.

Are Type l Channels the Same as g_{f2} Channels in Node of Ranvier?

In light of the additional information presented here, we have compared the type *l* K^+ channel with other types of K^+ channels described in the literature. Taking into account all known properties, type *l* channels in lymphocytes most closely resemble one of the two "fast" K^+ channels in frog node of Ranvier: the "g_{f2}" channel (Dubois, 1981*b*), also called the "*F*" channel (Jonas et al., 1989). These two K^+ channels are compared in detail in Table III. Considering differences in experimental milieu, the two channels are virtually identical with respect to all parameters for which quantitative comparisons can be made. We conclude that type *l* K^+ channels in lymphocytes are essentially identical to the g_{f2} K^+ channel in myelinated nerve. Considering the facility of the lymphocyte preparation and the abundance of type *l* K^+ channels in *lpr* T lymphocytes with only a small contaminant from other ion channels, while node of Ranvier has substantial contamination by two other K^+ channels, *lpr* lymphocytes may be the ideal preparation in which to study this type of K^+ channel.

We thank Dr. Fred N. Quandt for reading and commenting on this manuscript.

This work was supported by research grant HL-37500 (T. DeCoursey), Research Career Development Award KO4-1928 (T. DeCoursey), and NRSA pre-doctoral training grant HL-07320 (M. Shapiro) all from the National Institutes of Health.

The work presented here was part of that submitted by M. Shapiro in partial fulfillment of the degree of Ph.D.

Original version received 8 June 1990 and accepted version received 3 December 1990.

REFERENCES

Adams, D. J., W. Nonner, T. M. Dwyer, and B. Hille. 1981. Block of endplate channels by permeant cations in frog skeletal muscle. *Journal of General Physiology.* 78:593–615.

Århem, P. 1980. Effects of rubidium, caesium, strontium, barium and lanthanum on ionic currents in myelinated nerve fibres from *Xenopus laevis*. *Acta Physiologica Scandinavica.* 108:7–16.

Almers, W., and C. M. Armstrong. 1980. Survival of K^+ permeability and gating currents in squid axons perfused with K^+-free media. *Journal of General Physiology.* 75:61–78.

Altman, A., A. N. Theofilopoulos, R. Weiner, D. H. Katz, and F. J. Dixon. 1981. Analysis of T cell function in autoimmune murine strains. Defects in production of and responsiveness to interleukin 2. *Journal of Experimental Medicine.* 154:791–808.

Armstrong, C. M. 1975. Potassium pores of nerve and muscle membranes. *In* Membranes: A Series of Advances. G. Eisenman, editor. Marcel Dekker, Inc., New York. 325–358.

Armstrong, C. M., and F. Bezanilla. 1974. Charge movement associated with the opening and closing of the activation gates of the Na channels. *Journal of General Physiology.* 63:533–552.

Armstrong, C. M., and J. Lopez-Barneo. 1987. External calcium ions are required for postassium channel gating in squid neurons. *Science.* 236:712–714.

Armstrong, C. M., and D. R. Matteson. 1986. The role of calcium ions in the closing of K channels. *Journal of General Physiology.* 87:817–832.

Bezanilla, F., and C. M. Armstrong. 1982. Negative conductance caused by entry of sodium and cesium ions into the potassium channels of squid axons. *Journal of General Physiology.* 60:588–608.

Cahalan, M. D., K. G. Chandy, T. E. DeCoursey, and S. Gupta. 1985. A voltage-gated potassium channel in human T lymphocytes. *Journal of Physiology.* 358:197–237.

Chandler, W. K., and H. Meves. 1970. Sodium and potassium currents in squid axons perfused with fluoride solutions. *Journal of Physiology.* 211:623–652.

Chandy, K. G., T. E. DeCoursey, M. Fischbach, N. Talal, M. D. Cahalan, and S. Gupta. 1986. Altered K^+ channel expression in abnormal T lymphocytes from mice with the *lpr* gene mutation. *Science.* 233:1197–1200.

Clay, J. R., and M. F. Shlesinger. 1983. Effects of external cesium and rubidium on outward potassium currents in squid axons. *Journal of General Physiology.* 42:43–53.

Coronado, R., R. Latorre, and H. G. Mautner. 1984. Single potassium channels with delayed rectifier behavior from lobster axon membranes. *Biophysical Journal.* 45:289–299.

DeCoursey, T. E., K. G. Chandy, S. Gupta, and M. D. Cahalan. 1984. Voltage-gated K^+ channels in human T lymphocytes: a role in mitogenesis? *Nature.* 307:465–468.

DeCoursey, T. E., K. G. Chandy, S. Gupta, and M. D. Cahalan. 1987*a*. Two types of potassium channels in murine T lymphocytes. *Journal of General Physiology.* 89:379–404.

DeCoursey, T. E., K. G. Chandy, S. Gupta, and M. D. Cahalan. 1987*b*. Mitogen induction of ion channels in murine T lymphocytes. *Journal of General Physiology.* 89:405–420.

DeCoursey, T. E., E. R. Jacobs, and M. R. Silver. 1988. Potassium currents in rat type II alveolar epithelial cells. *Journal of Physiology.* 395:487–505.

Drouin, H., and R. The. 1969. The effect of reducing extracellular pH on the membrane currents of the Ranvier node. *Pflügers Archiv.* 313:80–88.

Dubois, J. M. 1981*a*. Simultaneous changes in the equilibrium potential and potassium conductance in voltage clamped Ranvier node in the frog. *Journal of Physiology.* 318:279–295.

Dubois, J. M. 1981*b*. Evidence for the existence of three types of potassium channels in the frog Ranvier node membrane. *Journal of Physiology.* 318:297–316.

Dubois, J. M. 1982. Capsaicin blocks one class of K^+ channels in the frog node of Ranvier. *Brain Research.* 245:372–375.

Gay, L. A., and P. R. Stanfield. 1978. The selectivity of the delayed potassium conductance of frog skeletal muscle fibers. *Pflügers Archiv.* 378:177–179.

Gilbert, D. L., and G. Ehrenstein. 1969. Effect of divalent cations on potassium conductance of squid axons: determination of surface charge. *Biophysical Journal.* 9:447–463.

Gilly, W. F., and C. M. Armstrong. 1982. Slowing of sodium channel opening kinetics in squid axon by extracellular zinc. *Journal of General Physiology.* 79:935–964.

Grissmer, S., M. D. Cahalan, and K. G. Chandy. 1988. Abundant expression of type *l* K^+ channels. *Journal of Immunology.* 141:1137–1142.

Hadley, R. W., and J. R. Hume. 1990. Permeation of Cs^+, Na^+, NH_4^+, and Rb^+ through the delayed rectifier in guinea-pig ventricular myocytes. *Biophysical Journal.* 57:141*a*. (Abstr.)

Hamill, O. P., A. Marty, E. Neher, B. Sakmann, and F. J. Sigworth. 1981. Improved patch-clamp techniques for high-resolution current recording from cells and cell-free membrane patches. *Pflügers Archiv.* 391:85–100.

Henderson, P. 1907. Zur Thermodynamik der Flüssigskeitsketten. *Zeitschrift der Physische Chemie.* 59:118–127.

Hille, B. 1968. Charges and potentials at the nerve surface. Divalent ions and pH. *Journal of General Physiology.* 51:221–236.

Hille, B. 1973. Potassium channels in myelinated nerve: selective permeability to small cations. *Journal of General Physiology.* 61:669–686.

Hille, B. 1975. Ionic selectivity, saturation, and block in sodium channels. *Journal of General Physiology.* 66:535–560.

Hille, B., and W. Schwarz. 1978. Potassium channels as multi-ion single-file pores. *Journal of General Physiology.* 72:409–442.

Hodgkin, A. L., and A. F. Huxley. 1952. A quantitative description of membrane current and its application to conduction and excitation in nerve. *Journal of Physiology.* 117:500–544.

Hu, S., and N. Rubly. 1983. Effects of morphine on ionic currents in frog node of Ranvier. *European Journal of Pharmacology.* 95:185–192.

Ilyin, V. I., I. E. Katina, A. V. Lonskii, V. S. Makovsky, and E. V. Polishchuk. 1980. The Cole-Moore effect in nodal membrane of the frog *Rana ridibunda:* evidence for fast and slow potassium channels. *Journal of Membrane Biology.* 57:179–193.

Jonas, P., M. E. Brau, M. Hermsteiner, and W. Vogel. 1989. Single-channel recording in myelinated nerve fibers reveals one type of Na channel but different K channels. *Proceedings of the National Academy of Sciences, USA.* 86:7238–7242.

Kawa, K. 1987. Transient outward currents and changes of their gating properties after cell activation in thrombocytes of the newt. *Journal of Physiology.* 385:189–205.

Lewis, R. S., and M. D. Cahalan. 1988. Subset-specific expression of potassium channels in developing murine T lymphocytes. *Science.* 239:771–775.

Lucero, M. T., and P. A. Pappone. 1989. Voltage-gated potassium channels in brown fat cells. *Journal of General Physiology.* 93:451–472.

Matteson, D. R., and C. Deutsch. 1984. K channels in T lymphocytes: a patch clamp study using monoclonal antibody adhesion. *Nature.* 307:468–471.

Matteson, D. R., and R. P. Swenson, Jr. 1986. External monovalent cations that impede the closing of K^+ channels. *Journal of General Physiology.* 87:795–816.

Mozhayeva, G. N., and A. P. Naumov. 1972. Influence of the surface charge on the steady potassium conductivity of the membrane of a node of Ranvier. III. Effect of bivalent cations. *Biofizika.* 17:801–808.

Murphy, E. E. 1981. Lymphoproliferation (*lpr*) and other single-locus models for murine lupus. *In* Immunologic Defects in Laboratory Animals. M. E. Gershwin and B. Merchant, editors. Plenum Publishing Corp., New York. 2:143–173.

Palti, Y., G. Ganot, and R. Stämpfli. 1976. Effect of conditioning potential on potassium current kinetics in the frog node. *Biophysical Journal.* 16:261–273.

Pickard, W. F., J. Y. Lettvin, J. W. Moore, M. Takata, J. Pooler, and T. Bernstein. 1964. Caesium ions do not pass the membrane of the giant axon. *Proceedings of the National Academy of Sciences, USA.* 52:1177–1183.

Plant, T. D. 1986. The effects of rubidium ions on components of the potassium conductance in the frog node of Ranvier. *Journal of Physiology.* 375:81–105.

Rae, J. L., and R. A. Levis. 1984. Patch voltage clamp of lens epithelial cells: theory and practice. *Molecular Physiology.* 6:115–162.

Reuter, H., and C. F. Stevens. 1980. Ion conductance and ion selectivity of potassium channels in snail neurones. *Journal of Membrane Biology.* 57:103–118.

Robinson, R. A., and R. H. Stokes. 1965. Electrolyte Solutions. Butterworths, London.

Röper, J., and J. R. Schwarz. 1989. Heterogeneous distribution of fast and slow potassium channels in myelinated nerve fibers. *Journal of Physiology.* 416:93–110.

Sands, S. B., R. S. Lewis, and M. D. Cahalan. 1989. Charybdotoxin blocks voltage-gated K^+ channels in human and murine T lymphocytes. *Journal of General Physiology.* 93:1061–1074.

Schwarz, J. R., and W. Vogel. 1971. Potassium inactivation in single myelinated nerve fibers of *Xenopus laevis*. *Pflügers Archiv.* 330:61–73.

Shapiro, B. I. 1977. Effects of strychnine on the potassium conductance of the frog node of Ranvier. *Journal of General Physiology.* 69:897–914.

Shapiro, M. S. 1990. Are type *l* K^+ channels in lymphocytes the same as g_{f2} K^+ channels in frog node of Ranvier? *Biophysical Journal.* 57:515*a*. (Abstr.)

Shapiro, M. S., and T. E. DeCoursey. 1988. Two types of potassium channels in a lymphoma cell line. *Biophysical Journal.* 53:550*a*. (Abstr.)

Shapiro, M. S., and T. E. DeCoursey. 1989. Selectivity and permeant ion effects on gating in type *l* K^+ channels. *Biophysical Journal.* 55:200*a*. (Abstr.)

Shapiro, M. S., and T. E. DeCoursey. 1991. Permeant ion effects on the gating kinetics of the type *l* potassium channel in mouse lymphocytes. *Journal of General Physiology.* 97:1251–1278.

Shibasaki, T. 1987. Conductance and kinetics of delayed rectifier potassium channels in nodal cells of the rabbit heart. *Journal of Physiology.* 387:227–250.

Spruce, A. E., N. B. Standen, and P. R. Stanfield. 1989. Rubidium ions and the gating of delayed rectifier potassium channels of frog skeletal muscle. *Journal of Physiology.* 411:597–610.

Swenson, R. P., Jr., and C. M. Armstrong. 1981. K^+ channels close more slowly in the presence of external K^+ and Rb^+. *Nature.* 291:427–429.

Vanýsek, P. 1987. Equivalent ionic conductivities extrapolated to infinite dilution in aqueous solutions at 25°C. *In* CRC Handbook of Chemistry and Physics. R. C. Weast, editor. CRC Press, Boca Raton, FL. D-167–D-169.

Wagoner, P. K., and G. S. Oxford. 1987. Cation permeation through the voltage-dependent potassium channel in the squid axon. *Journal of General Physiology.* 90:261–290.

Wofsy, D. E., D. Murphy, J. B. Roths, M. J. Duaphinee, S. B. Kipper, and N. Talal. 1981. Deficient interleukin 2 activity by MRL/Mp and C57BL/6J mice bearing the *lpr* gene. *Journal of Experimental Medicine.* 154:1671–1680.

Woodhull, A. M. 1973. Ionic blockage of sodium channels in nerve. *Journal of General Physiology.* 61:687–708.